THE JOURNAL OF BIOLOGICAL CHEMISTRY VOL. 287, NO. 6, pp. 4053–4065, February 3, 2012

Glioma-specific Cation Conductance Regulates Migration and Cell Cycle Progression*[S]

Received for publication, October 7, 2011, and in revised form, November 18, 2011 Published, JBC Papers in Press, November 30, 2011, DOI 10.1074/jbc.M111.311688

Arun K. Rooj[‡], Carmel M. McNicholas[‡], Rafal Bartoszewski[§], Zsuzsanna Bebok[§], Dale J. Benos[‡§†], and Catherine M. Fuller[‡§1]

From the Departments of [‡]Physiology and Biophysics and [§]Cell Biology, University of Alabama at Birmingham, Birmingham, Alabama 35294

Background: Cation transport contributes to migration and proliferation of tumor cells.
Results: Sodium current block decreased ERK phosphorylation and increased expression of cell cycle inhibitors.
Conclusion: Activity of an ENaC/ASIC cation channel is required to maintain the glioma cell phenotype.
Significance: Activity of a membrane cation channel influences signaling pathways to effect changes in migration and proliferation of glioma cells.

In this study, we have investigated the role of a glioma-specific cation channel assembled from subunits of the Deg/epithelial sodium channel (ENaC) superfamily, in the regulation of migration and cell cycle progression in glioma cells. Channel inhibition by psalmotoxin-1 (PcTX-1) significantly inhibited migration and proliferation of D54-MG glioma cells. Both PcTX-1 and benzamil, an amiloride analog, caused cell cycle arrest of D54-MG cells in G_0/G_1 phases (by 30 and 40%, respectively) and reduced cell accumulation in S and G_2/M phases after 24 h of incubation. Both PcTX-1 and benzamil up-regulated expression of cyclin-dependent kinase inhibitor proteins $p21^{Cip1}$ and $p27^{Kip1}$. Similar results were obtained in U87MG and primary glioblastoma multiforme cells maintained in primary culture and following knockdown of one of the component subunits, ASIC1. In contrast, knocking down δENaC, which is not a component of the glioma cation channel complex, had no effect on cyclin-dependent kinase inhibitor expression. Phosphorylation of ERK1/2 was also inhibited by PcTX-1, benzamil, and knockdown of ASIC1 but not δENaC in D54MG cells. Our data suggest that a specific cation conductance composed of acid-sensing ion channels and ENaC subunits regulates migration and cell cycle progression in gliomas.

Glioblastoma multiforme (GBM),[2] a grade IV primary brain tumor, is the most common and aggressive of all brain tumors, exhibiting high rates of proliferation and migration, often setting up secondary foci some distance from the primary site. Ion channel activity is closely linked to changes in proliferation and migration of tumor cells (1–3), although the role of ion channels in the mechanisms underlying these processes is not well understood. There is increasing evidence that expression of Ca^{2+}, K^+, and Cl^- (4–6) channels is altered in many cancer cells and that the cellular pathophysiology is influenced by abnormal activities of these channels. Other basic phenotypic characteristics of tumor cells, such as cell adhesion (7) and interaction with the extracellular matrix (8), are also influenced by ion channel activity. Regulation of these parameters in both normal and tumor cells is also under the control of a diverse array of signaling pathways. Chief among these is the mitogen-activated protein kinase (MAPK) pathway, which regulates glioma cell migration, proliferation, and differentiation (9, 10). A key downstream signaling element of this pathway is the highly pluripotent signaling intermediate ERK1/2. Activation of this pathway is generally attributed to ligand binding to EGFR and related receptors, initiating a classical tyrosine kinase signaling cascade. In epithelial cells, ERK activation is associated with decreased surface expression of ENaC sodium channels (11, 12), exerting effects on mechanisms of channel retrieval from the membrane.

We have previously shown that malignant glioma cells express an inward Na^+ current that is not detected in normal astrocytes or low grade gliomas and is blocked by the diuretic amiloride (13). This cation current is due to expression of a cross-clade channel composed of members of the Deg/ENaC channel superfamily, *i.e.* acid-sensitive ion channel 1 (ASIC1) and two members of the epithelial sodium channel family, α- and γENaC (13–16). The amiloride-sensitive cation conductance found in glioma cells is also blocked by psalmotoxin-1 (PcTX-1), a peptide isolated from West Indies tarantula *Psalmopoeus cambridgei* (17, 18), and is a highly specific blocker of ASIC1. Knocking down expression of any of the three Deg/ENaC subunits abolishes the current and slows migration (15). Furthermore, the regulatory volume increase of glioma cells following cell shrinkage by hyperosmolar solutions was completely abolished by PcTX-1 and amiloride (19). Based on these previous findings, we wanted to determine whether PcTX-1 could affect glioma cell migration and proliferation. We report here that exposure to PcTX1, an amiloride analog benzamil, low extracellular [Na^+], or knockdown of the ASIC1 subunit

* This work was supported, in whole or in part, by National Institutes of Health Grant DK37206.
[S] This article contains supplemental Figs. S1–S5.
† Deceased, October 7, 2010.
[1] To whom correspondence should be addressed: Dept. of Physiology and Biophysics, MCLM 830, University of Alabama at Birmingham, 1530 3rd Ave. South, Birmingham, AL 35294. Tel.: 205-934-6227; Fax: 205-975-7679; E-mail: cfuller@uab.edu.
[2] The abbreviations used are: GBM, glioblastoma multiforme; ASIC, acid-sensing ion channel; PcTX-1, psalmotoxin-1; CKI, cyclin-dependent kinase inhibitor; NHE, Na^+/H^+ exchanger; EGFR, EGF receptor; eGFP, enhanced GFP; ENaC, epithelial sodium.

reduced migration, caused accumulation of $p21^{Cip1}$ and $p27^{Kip1}$ slowing proliferation, and decreased phosphorylation of ERK1/2 in two tumor cell lines, D54-MG and U87-MG, and in GBM cells maintained in primary culture. These observations reveal that activity of this channel is essential for the maintenance of the glioma cell phenotype.

EXPERIMENTAL PROCEDURES

Cell Culture—The cell line, D54-MG, and primary cultures of human glioblastoma cells were kind gifts of Dr. D. Bigner (Duke University, Durham, NC) and Dr. G. Y. Gillespie (University of Alabama at Birmingham, Neurosurgery Brain Tissue Bank). U87-MG cells were purchased from ATCC. The cells were cultured and maintained in Dulbecco's modified Eagle's/F-12 medium (Invitrogen) supplemented with 10% fetal bovine serum (Thermo-Fisher) in the absence of antibiotics. To generate stable cell lines, D54-MG cells were transfected with 4 μg of a truncated eGFP-ASIC1 or eGFP-δENaC cDNA as described previously (15). Following transfection, cells were cultured for 72 h, transferred to a T75 flask, and selected with G418 (500 μg/ml; Mediatech, Manassas, VA). After initial selection, GFP-positive cells were sterile sorted by FACS. Stable transfectants were maintained in DMEM/F-12 media with 10% FBS. All constructs used were the human variants, subcloned into pcDNA3.1 for expression.

Transwell Migration Assay—Transwell migration assays were conducted as described previously (16). Cells were split 1 day prior to the experiment and treated with PcTX-1 (100 nM), control peptide (100 nM) (Peptides International, Louisville, KY), or benzamil (100 μM) (Sigma). These drug concentrations were used for all subsequent experiments. The control peptide had an identical amino acid sequence as PcTX-1 except all the cysteines were replaced with alanine, thus breaking the disulfide bonds of this inhibitor cysteine knot fold toxin. On the day of the experiment, 1×10^4 cells were added to the insert and allowed to migrate for 5 h (37 °C, 95% air, 5% CO_2), in the continued presence of the drugs, which were added to both sides of the filter. Following incubation, cells were fixed (4% paraformaldehyde) for 10 min and stained with 1% crystal violet solution (5 min). Images from five random fields per insert were taken at ×20 magnification. All experiments were done in triplicate and repeated a minimum of three times per condition.

Scratch Wound Migration Assay—D54-MG cells (either wild type or stably transfected with truncated eGFP-ASIC1) were seeded on a 6-well plate at a density of 7×10^5 cells/well. The monolayer was scarred with a 200-μl sterile pipette tip and washed two times with serum-free DMEM/F-12 media. Immediately after scarring, cells were treated with PcTX-1, control peptide, or benzamil for 24 h (DMEM/F-12 with 2% FBS) at 37 °C. Images were taken at 0 h and after 24 h of treatment, and the cell-free area was measured. The experiments were performed at least three times per condition. Images were captured on a Nikon 200 TEV inverted microscope. IPLab software was used to measure the region of interest in the scratch area.

Isolation of Cellular RNA—Total cellular RNA was isolated from D54-MG cells using RNeasy (Qiagen, Valencia, CA), according to the manufacturer's recommendations. RNA was isolated from D54-MG cells treated with PcTX-1 (100 nM) or control peptide (100 nM) or benzamil (100 μM) or incubated in DMEM/F-12 (with 2 or 10% FBS) or Kreb's buffer or $NMDG^+$ buffer for 24 h or from D54MG cells stably transfected with either DN-eGFP-ASIC1 cDNA or DN-eGFP-δENaC cDNA. RNA concentration was calculated based on the absorbance at 260 nm. RNA samples were stored at −20 °C.

Measurement of Relative mRNA Levels Using Real Time PCR—Real time PCR to measure p21 (Hs00355782_m1) and p27 (Hs00153277_m1) mRNA was performed using TaqMan® One-step RT-PCR Master Mix reagents (Applied Biosystems, Carlsbad, CA) according to the manufacturer's directions (Relative Quantification, Applied Biosystems 7300/7500 Real Time PCR system). 18 S rRNA (Hs99999901_m1) was amplified as an internal control and used as a reference.

Flow Cytometry—Cells were seeded in a 6-well plate at a density of 2×10^5/well. After 24 h, the cells were washed three times with PBS and then incubated with serum-free DMEM/F-12 for 48 h to synchronize the cells in G_0/G_1 phase. The cells were incubated with either PcTX-1, control peptide, or benzamil for 24 h in reduced serum media (DMEM/F-12 with 2% FBS) at 37 °C. After fixing with 95% ethanol, the cells were treated with RNase solution (1 mg/ml in PBS; Thermo-Fisher), stained with propidium iodide (40 μg/ml) (Sigma), and sorted at the FACS core facility in the Center for AIDS Research (University of Alabama at Birmingham). Cell cycle phases were analyzed by FACS-Diva software (BD Biosciences).

Cell Lysates, SDS-PAGE, and Immunoblotting—Cells were washed twice with cold PBS and lysed in buffer (150 mM NaCl, 5 mM EDTA, 50 mM Tris, pH 7.4, 1% Triton X-100, Complete® protease inhibitor mixture (Roche Applied Science)) for 30 min at 4 °C with shaking. Cell lysates were homogenized by passing 10 times through a 22-gauge needle and centrifuged (13,200 rpm for 30 min at 4 °C). Protein concentration of the supernatant was measured using BCA protein assay (Thermo-Scientific), and 25–50 μg of protein lysates were used per lane for SDS-PAGE and immunoblotting. Lysates were heated at 95 °C for 6–7 min in 1× Laemmli sample buffer (25% glycerol, 2% SDS, 0.01% bromphenol blue, 10% β-mercaptoethanol, 62.5 mM Tris-HCl, pH 6.8) and subjected to SDS-PAGE over 8 or 12% separating gels. Proteins were transferred to Immobilon-P transfer membranes (Millipore, Hayward, CA). Following transfer, membranes were blocked for 1 h with 5% nonfat dry milk or 10% BSA (for phosphor-specific antibody) in Tris-buffered saline (100 mM Tris, pH 7.5), 150 mM NaCl), with Tween 20 (0.1%, Bio-Rad; TBS-T) for 1 h at room temperature and probed with primary antibodies in 5% milk or 10% BSA in TBS-T overnight at 4 °C. Blots were washed with TBS-T (three times for 5 min), and probed with secondary antibodies conjugated to horseradish peroxidase (HRP; Thermo-Fisher) in 5% milk in TBS-T. The blots were developed in SuperSignal West Pico substrate (Thermo-Fisher) and exposed to x-ray film. The x-ray films were scanned using a Syngene G-Box, and images were analyzed for densitometry by GeneTools software (Syngene).

Antibodies and Drugs—The following antibodies were used: mouse anti-GFP monoclonal antibody (Abgent, San

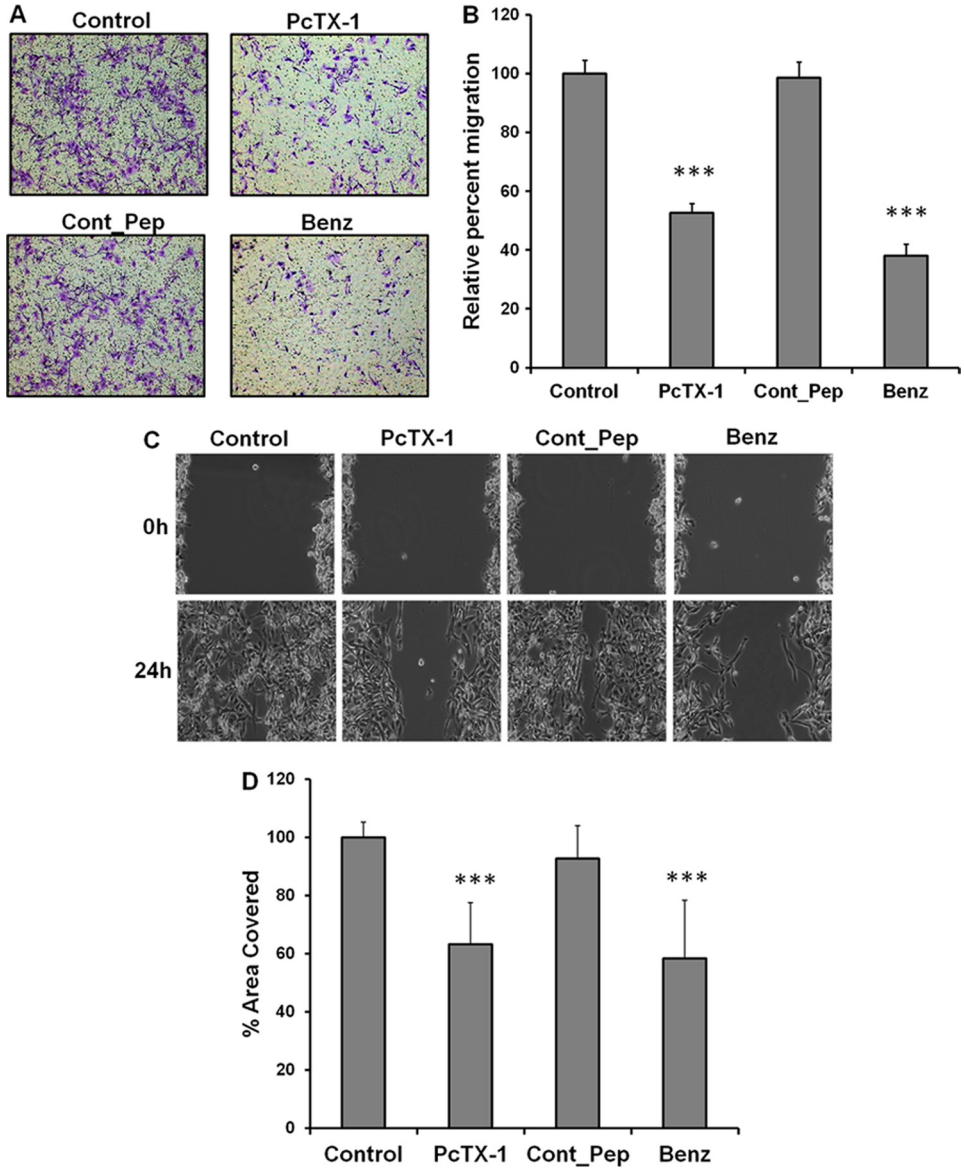

FIGURE 1. **Inhibition of ASIC-1 by PcTX-1 reduces migration and proliferation of D54-MG glioma cells.** *A,* representative microscopic images of transwell filters, showing migration of D54-MG cells following a 24-h exposure to PcTX-1, control peptide (*Cont_Pep*), or benzamil (*Benz*). Drugs were present on both sides of the filter throughout the 5-h migration period. In each experiment, the number of cells on the underside of the filter was counted from five randomly selected fields of each image ($n \geq 3$). *B, bar graph* showing the average number of migrated cells per field under each condition (normalized to control). *C,* scratch/wound assay. Phase contrast image of D54-MG cells untreated or treated with PcTX-1, control peptide, or benzamil at 0 and 24 h after scarring. *D,* summary *bar graph* showing results expressed as % wound area covered at 24 h, normalized to control conditions ($n \geq 4$).

Diego) at 1:2000; mouse anti-p21 monoclonal antibody (Abcam, Cambridge, MA) at 1:2000; mouse anti-p27 monoclonal antibody (Cell Signaling, Danvers, MA) at 1:1000; rabbit anti-ERK1/2 polyclonal antibody (Millipore) at 1:10,000; mouse anti-phospho-ERK1/2 monoclonal antibody (Millipore) at 1:10,000; rabbit anti-ASIC1 and anti-δENaC (Santa Cruz Biotechnology, Santa Cruz, CA) at 1:500; and mouse anti-actin monoclonal antibody (Millipore) at 1:200,000. Because glioma cells release proteases, we used PcTX-1 (and control peptide) at 100 nM for long term (24 h) inhibition of the glioma-specific cation conductance. Similarly, we conducted experiments at reduced (2%) serum concentrations to limit binding of the toxin to plasma proteins. Benzamil and amiloride were used at 100 μM.

Electrophysiology—Whole-cell current recordings were obtained using the amphotericin B perforated patch technique as described previously (20). Cells were mounted in a flow-through chamber on the stage of a Leica DM IRB inverted microscope (Leica Microsystems, Heidelberg, Germany). Bath solution exchange was achieved using a pinch valve control system converging on an 8-1 manifold. Tips of borosilicate recording pipettes (5–7 megohms) were back-filled with pipette solution (150 mM KCl, 10 mM HEPES, pH 7.2 (Tris-HCl)) and then with the same solution containing ~0.2 mg/ml amphotericin B (Sigma). Currents were obtained using an Axopatch 200B patch clamp amplifier (Axon Instruments/Molecular Devices, Sunnyvale, CA) with voltage commands and data acquisition controlled by Clampex software (pClamp 8, Axon

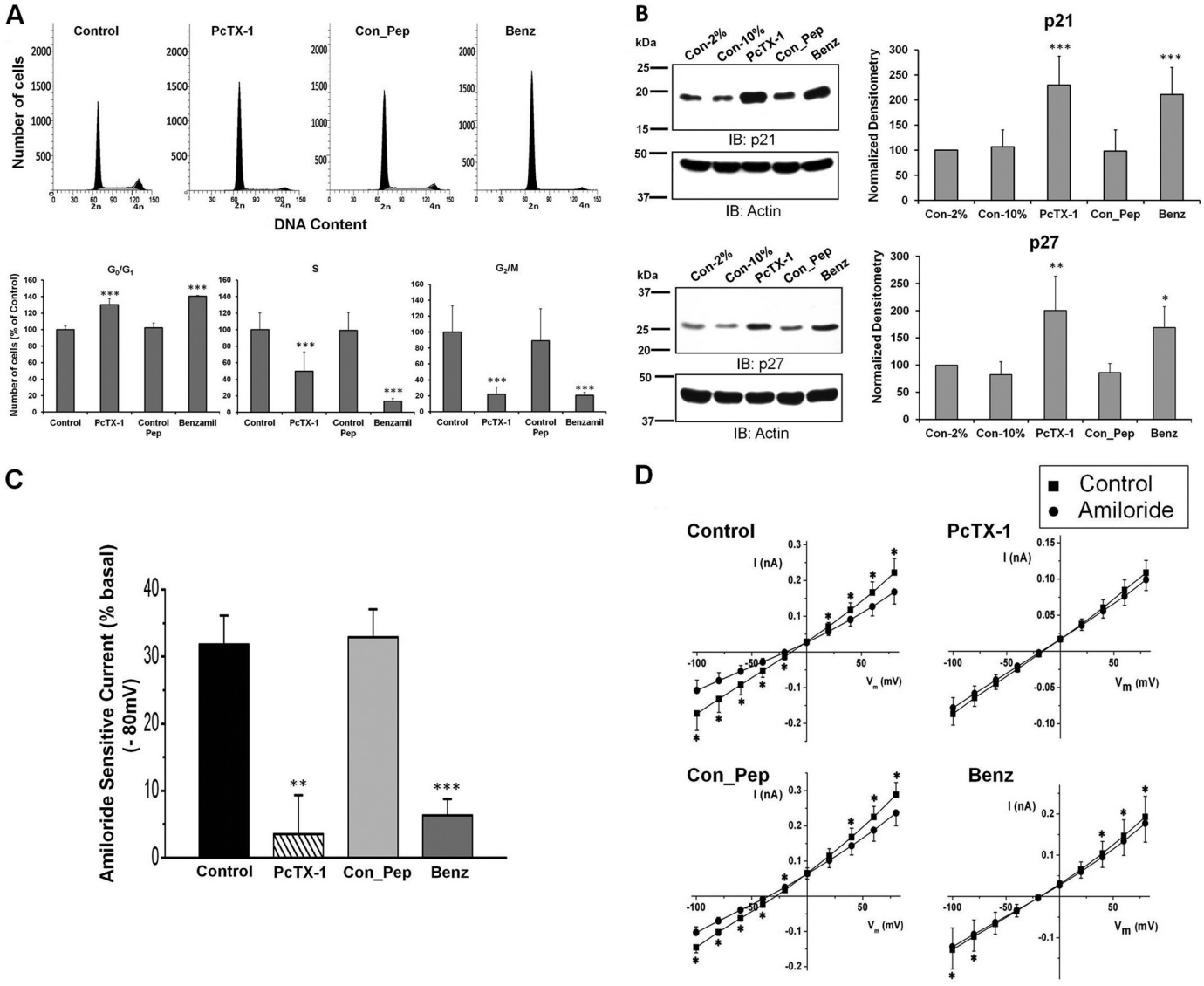

FIGURE 2. **Effect of inhibition of ASIC-1 on cell cycle progression and whole-cell current of D54-MG glioma cells.** *A,* flow cytometric analysis of D54-MG cells treated with PcTX-1, control peptide (*Con_Pep*), and benzamil (*Benz*) for 24 h. DNA content is shown as 2*n* and 4*n* in the *x* axis where 2*n* = cells in G_0/G_1 phase and 4*n* = cells in G_2/M phase. The *bar graph* shows the percentage of cells in each cell cycle phase for the different experimental conditions, $n \geq 4$. *B,* expression of $p21^{Cip1}$ and $p27^{Kip1}$ proteins in D54-MG cells treated with PcTX-1, control peptide, or benzamil for 24 h. β-Actin was used as a loading control. Accompanying *bar graph* shows the normalized density as compared with 2% FBS control $n \geq 6$. *IB*, immunoblot. *C, bar graph* showing average amiloride-sensitive currents at −80 mV for D54-MG cells pretreated with PcTX-1, control peptide, or benzamil for 24 h. Currents were recorded in the continued presence of drug in the bath solution $n \geq 6$. *D,* summary *I/V* curves showing basal current and that following addition of amiloride to the bath solution.

Instruments) and digitized (Digidata 1321A interface, Axon Instruments) at a sampling frequency of 2 kHz. Current-voltage relationships were obtained using a pulse protocol in which cells were stepped from a −40-mV holding potential from −100 to +80 mV in 20-mV increments for 250 ms. Mean currents were obtained from the average of three sweeps during the 200–250-ms period of each sweep using Clampfit 8 software (Axon Instruments). Bath solutions contained (in mM) 140 NaCl, 4.0 KCl, 1.8 $CaCl_2$, 1.0 $MgCl_2$, 10 glucose, 10 HEPES, pH 7.4 (NaOH/HCl). Appropriate vehicle controls were performed.

Data Analysis and Statistics—Statistical analysis was done with Microsoft Excel or GraphPad Prism 5. All experiments were performed at least three times. Statistical significance is displayed on the figure according to the level of significance (*, $p < 0.05$; **, $p < 0.01$; ***, $p < 0.001$). Data are presented as means ± S.D., and two-tailed *t* tests (unpaired or paired) were performed for two group comparisons, and one-way analysis of variance followed by post hoc tests were used to compare three or multiple groups.

RESULTS

PcTX-1 Inhibits Migration and Proliferation of D54-MG Glioma Cells—As ASIC-1 is one subunit of the glioma-specific heteromeric ion channel complex, we wanted to determine whether prolonged (24 h) inhibition of the cation conductance by PcTX-1 affected the migration of D54-MG cells. If the channel is crucial for the migratory phenotype of glioma cells, PcTX-1-treated D54-MG cells should show a lower rate of migration as compared with untreated cells or cells treated with the con-

trol peptide. As shown in Fig. 1, *A* and *B*, we found that PcTX-1 and benzamil significantly inhibited migration (by 48 ± 3 and 62 ± 4%, respectively, $n \geq 3$) as compared with untreated cells or cells treated with control peptide. Similarly, in the scratch wound/healing assay (Fig. 1, *C* and *D*), cells treated with PcTX-1 and benzamil had significantly lower rates of migration (by 37 ± 13 and 42 ± 18%, respectively, $n \geq 4$), than untreated cells or cells treated with control peptide.

PcTX-1 Causes Cell Cycle Arrest at G_0/G_1 Phase and Inhibition of Cation Current in D54-MG Glioma Cells—Because closure of the scratch reflects both cell migration and proliferation, we examined the effect of PcTX-1 on cell cycle progression in D54-MG cells. Using FACS analysis, we found cell cycle arrest in the G_0/G_1 phase in PcTX-1- and benzamil-treated cells by 30 ± 7.4 and 40 ± 1%, respectively, as compared with untreated cells or cells treated with control peptide (Fig. 2*A*; $n \geq 5$). The number of cells in S and G_2/M phases was concomitantly reduced, implying that the inhibition of the cation conductance directly influenced cell cycle progression. The cell cycle is regulated by different classes of cyclin-dependent kinases whose activities are controlled by CKIs (21). We therefore explored whether expression of two CKIs, $p21^{Cip1}$ and $p27^{Kip1}$, was also affected by the toxin. As shown in Fig. 2*B*, expression of both CKIs was significantly increased when D54-MG cells were treated with PcTX-1 or benzamil for 24 h. Reduction of FBS in the media to 2% to reduce binding of toxin to plasma proteins was without effect ($n \geq 6$).

We also verified that the amiloride-sensitive cation current that we had previously recorded from glioma cells was inhibited by long term exposure to PcTX-1 and benzamil. We found that ~32% ($n \geq 6$) of the total basal current at −80 mV was amiloride-sensitive in untreated cells (Fig. 2*C*). In contrast, in PcTX-1- and benzamil-preincubated cells, only 3.5 and 6.3%, respectively, of the remaining basal current was amiloride-sensitive, consistent with a nearly complete abrogation of current by the drugs. Under these conditions, the control peptide had no effect. The *I/V* relationships for each condition described above are shown in Fig. 2*D*. Representative individual whole-cell current records under each experimental condition are shown in supplemental Fig. 1.

Knockdown of ASIC-1 Expression Inhibits Migration and Cell Cycle Progression in D54-MG Cells—We generated a stable D54-MG cell line expressing an eGFP-tagged ASIC-1 construct (DN-eGFP-ASIC1), containing a premature stop mutation at Tyr-67 (Y67X). This construct effectively knocks down expression of endogenous ASIC1, but it does not affect expression of other related subunits (15). We analyzed whole-cell lysates obtained from both wild type D54-MG (D54MG-WT) cells and D54-MG cells stably transfected with the DN-eGFP-ASIC1 cDNA (D54MG-A1DN) for ASIC-1 protein expression. Quantitative densitometric analysis showed that the expression of ASIC-1 was significantly decreased by 58 ± 13% ($n \geq 4$) in D54MG-A1DN cells (Fig. 3*A*). Whole-cell patch clamp recording demonstrated that only 9% of basal current exhibited amiloride sensitivity in contrast to ~32% in the wild type cells ($n \geq 6$; Fig. 3, *B* and *C*). Representative individual whole-cell current records of wild type and stably transfected cells under each experimental conditions are shown in supplemental Fig. 2.

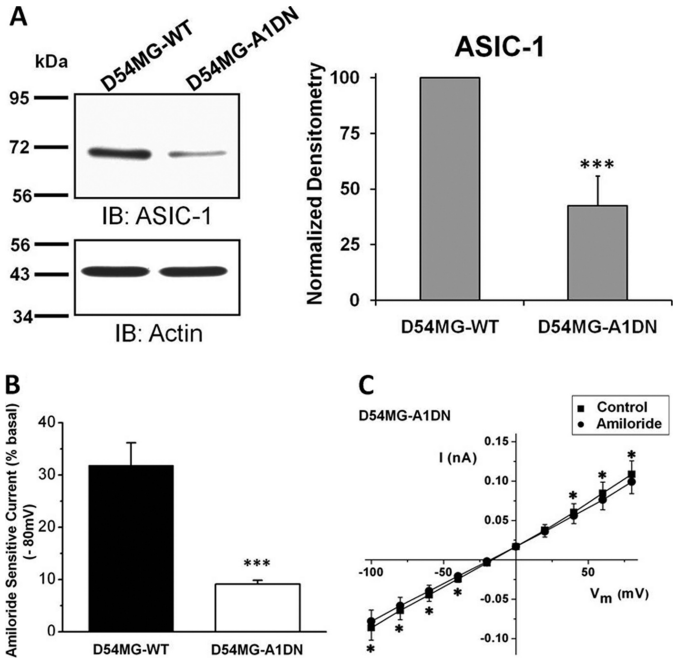

FIGURE 3. **Knockdown of ASIC1 expression inhibits amiloride-sensitive current in D54-MG glioma cells.** *A,* lysates from untransfected wild type D54-MG (*D54MG-WT*) and D54-MG cells stably transfected with DN-eGFP-ASIC1 cDNA (*D54MG-A1DN*) were analyzed. The expression of ASIC-1 was significantly decreased in D54MG-A1DN cells compared with wild type cells, $n \geq 6$. *IB*, immunoblot. *B,* average amiloride-sensitive currents at −80 mV, $n \geq 6$. *C, I/V* curves show significant attenuation of amiloride-sensitive whole-cell current after knocking down ASIC1.

We hypothesized that knocking down ASIC-1 in glioma cells would have similar inhibitory effects as long term inhibition of ASIC-1 by PcTX-1 or benzamil. In both transwell migration (Fig. 4*A*) and scratch/wound healing assays (Fig. 4*B*), D54MG-A1DN cells showed a significant reduction in migration (by 40 ± 5%, $n \geq 3$, and by 39 ± 16%, $n \geq 4$, respectively), as compared with wild type D54-MG cells.

Similarly, ASIC-1 knockdown inhibited progression through the cell cycle consistent with the results from our earlier experiments (Fig. 4*C*). After 48 h of serum starvation, exposing D54MG-A1DN cells to DMEM/F-12, 10% FBS for 24 h significantly increased the percentage of the cell population in the G_0/G_1 phase (by 19 ± 5%, $n \geq 3$), as compared with wild type cells. The percentage of cells in S and G_2/M phases was significantly decreased in D54MG-A1DN cells (by 29 ± 7 and 66 ± 18%, respectively, $n \geq 3$). Consistent with our FACS data, we also found that ASIC-1 knockdown significantly increased the expression of $p21^{Cip1}$ (by 3-fold, $n \geq 6$) and $p27^{Kip1}$ (by 2.5-fold, $n \geq 5$), as compared with the wild type cells (Fig. 4*D*). As we have shown previously that δENaC is not a part of the glioma cation channel complex as knocking down this subunit did not affect the amiloride-sensitive glioma cation current (15), we established a stable D54-MG glioma cell line expressing a GFP-tagged truncated (S35X) δENaC construct. Western blot analysis (Fig. 5*A*) of whole-cell lysates showed that the expression of both glycosylated (upper band ~100 kDa) and nonglycosylated (lower band ~75 kDa) forms of δENaC (22) was significantly reduced (by 50 ± 15%, $n \geq 3$) in D54MG-δENaC-DN cells as

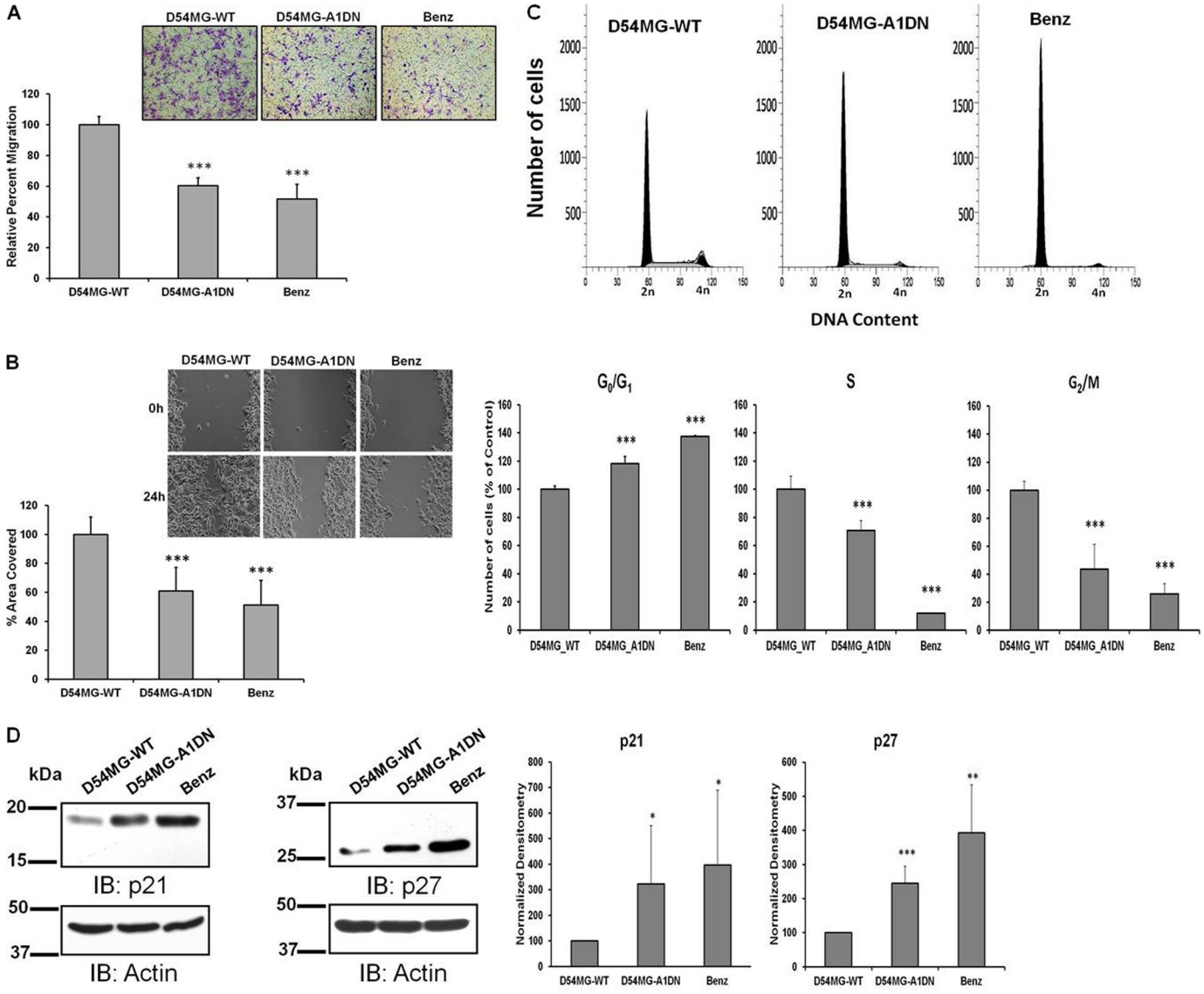

FIGURE 4. **Knockdown of ASIC1 inhibits migration and proliferation of D54-MG cells.** Summary data showing migration of untransfected D54MG-WT, D54MG-A1DN, and D54-MG-WT cells treated with benzamil (*Benz*) for 24 h and evaluated by transwell migration as described for Fig. 1 (*A*) and scratch/wound healing assay at 0 and 24 h after scarring $n \geq 4$ (*B*). *C*, flow cytometric analysis of D54MG-WT, D54MG-A1DN, and D54-MG cells treated with benzamil for 24 h; the percentage of cells in each cell cycle phase for different experimental conditions is shown $n \geq 3$. *D*, expression of $p21^{Cip1}$ ($n \geq 6$) and $p27^{kip1}$ ($n \geq 5$) was determined in D54MG-A1DN cells following re-feeding with 10% FBS after 48 h of serum starvation. Actin was used as a loading control. Each *bar* represents normalized densitometry compared with untransfected D54MG-WT cells. *IB*, immunoblot.

compared with D54MG-WT cells. Expression of $p21^{Cip1}$ and $p27^{Kip1}$ was similarly unaffected by knocking down δENaC (Fig. 5*B*).

We also repeated these experiments in wild type D54-MG cells under conditions of low (25 mM) external Na^+. Incubation with low $[Na^+]$ media increased the proportion of cells in G_0/G_1 phase as compared with those in normal buffer. The numbers of cells in subsequent S phase and G_2/M phases were correspondingly lower in cells incubated in NMDG buffer, indicating that the extracellular sodium concentration is a critical regulator of the cell cycle. As shown in Fig. 6, *A* and *B*, lowering the external sodium concentrations evoked essentially identical results to those for the D54MG-A1DN cells. The expression of $p21^{Cip1}$ ($n \geq 5$) and $p27^{Kip1}$ ($n \geq 4$) was significantly up-regulated when the cells were exposed to low $[Na^+]$ buffer as compared with control buffer. These findings suggest that disrupting Na^+ transport across the membrane by whatever mechanism inhibits cell migration and proliferation.

Inhibition of the Glioma Cation Conductance Decreases Phosphorylation of ERK1/2—The MAPK signaling cascade is a crucial intracellular regulatory pathway that controls diverse cellular processes, including cell proliferation, cell cycle progression, cell survival, and angiogenesis (9, 23). Our findings that glioma cell migration, proliferation, and the cell cycle were down-regulated by PcTX-1, benzamil, low extracellular $[Na^+]_o$, and by knocking down the expression of ASIC-1 prompted us to determine the phosphorylation status of ERK1/2 in all of our previous experimental conditions. We found that phosphorylation of ERK1/2 was significantly inhibited when we treated the cells with PcTX-1 (by 82 ± 22%, $n \geq 3$, or benzamil (by 82 ± 24%, $n \geq 3$), as compared with control cells (in 2% or 10% FBS)

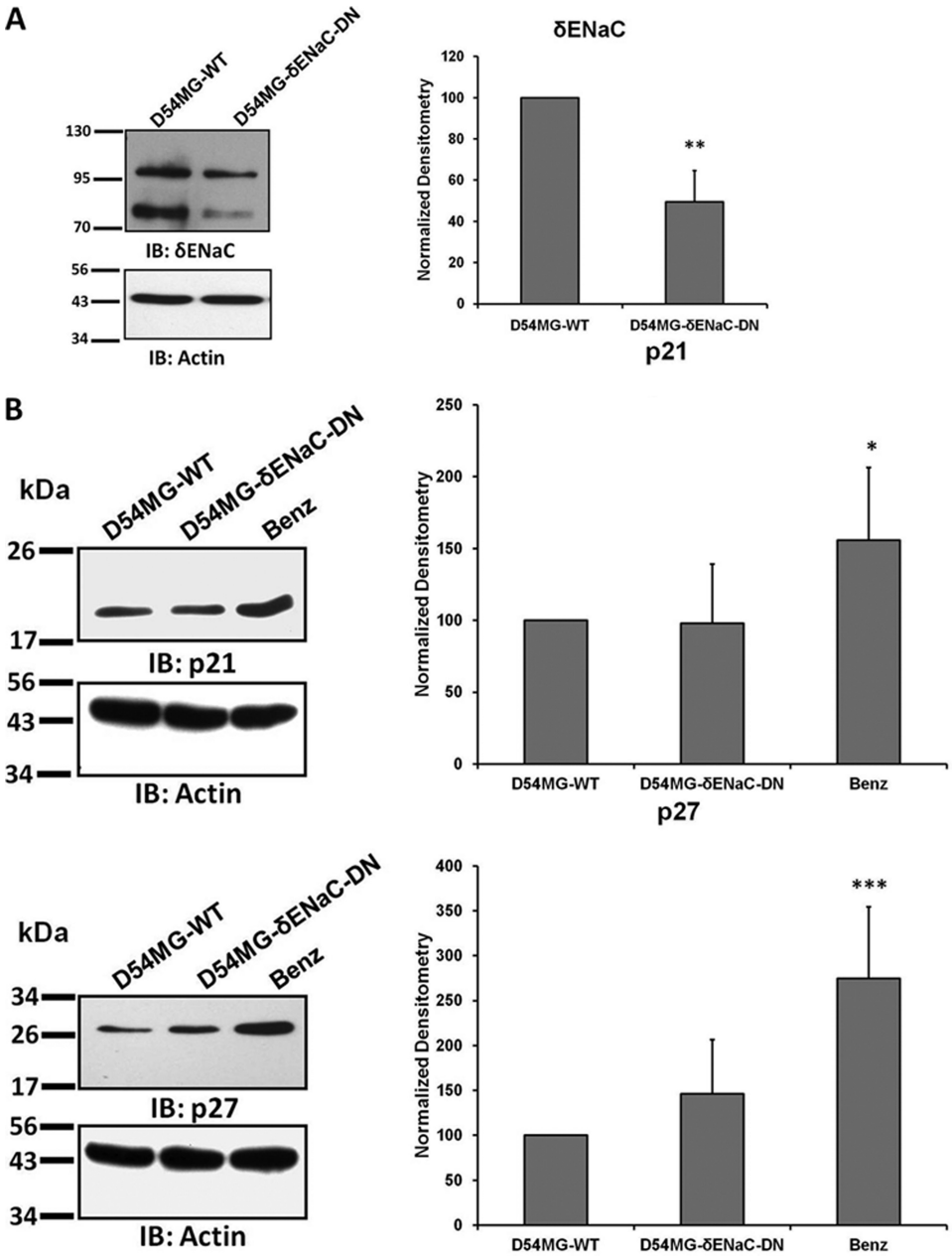

FIGURE 5. **Knocking down δENaC has no effect CKI expression.** *A,* lysates from untransfected wild type D54-MG and D54MG-δENaC-DN cells were separated by SDS-PAGE and immunoblotting (*IB*). Each *bar* represents the normalized density of both bands compared with untransfected D54-MG cells, $n \geq 3$. *B,* no difference in expression of $p21^{Cip1}$ and $p27^{kip1}$ proteins was detected between wild type D54-MG and D54MG-δENaC-DN cells. Wild type cells treated with benzamil were used as a positive control ($n \geq 6$).

or cells treated with control peptide (Fig. 7*A*). Stably knocking down ASIC-1 in D54-MG cells also significantly decreased ERK1/2 phosphorylation by 47 ± 20%, $n \geq 6$ (Fig. 7*B*). In contrast, knocking down δENaC in this glioma cell line had no effect on phosphorylation of ERK1/2 (Fig. 7*C*). Low $[Na^+]$ also down-regulated phosphorylation of ERK1/2 in D54-MG glioma cells following 24 h of incubation (Fig. 7*D*, $n \geq 4$). These findings suggest that normal channel activity is required for ERK1/2 phosphorylation.

Expression of $p21^{Cip1}$ and $p27^{Kip1}$ Is Increased and ERK1/2 Phosphorylation Is Decreased by PcTX1 and Benzamil in Primary GBM Cells—To determine whether our findings were more widely applicable, we evaluated the effect of current inhibition on cell cycle progression and ERK phosphorylation in primary GBM cells. Fig. 8*A* shows that there was a significantly higher percentage of cells in the G_0/G_1 phase following PcTX-1 and benzamil treatment (26%, $n \geq 6$, and 25%, $n \geq 6$), respectively, as compared with the controls. The percentage of cells in S and G_2/M phases was correspondingly reduced. As shown in Fig. 8*B*, expression of $p21^{Cip1}$ and $p27^{Kip1}$ in primary GBM cells was significantly increased by treatment with PcTX-1 and benzamil ($n \geq 5$). Similarly, the phosphorylation of ERK1/2 was significantly reduced in PcTX-1- (by 85 ± 5%, $n \geq 4$) or benzamil (by 79 ± 24%, $n \geq 4$)-treated primary GBM cells. Essentially identical results were obtained in the second cell line U87MG, with

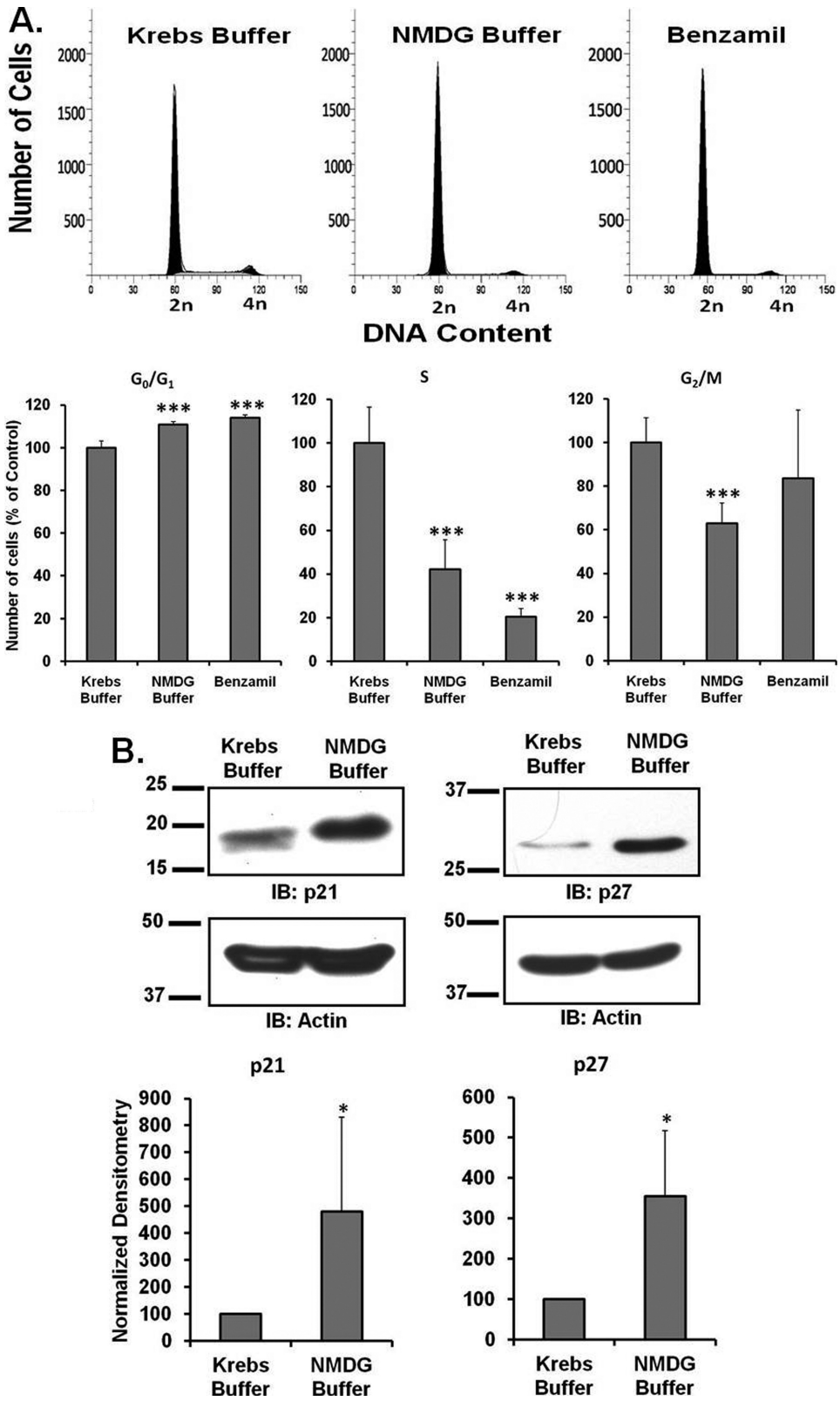

FIGURE 6. **Effect of low sodium on cell cycle progression of D54-MG glioma cells.** *A,* FACS analysis of D54-MG cells incubated in either control Krebs buffer (in mM: 118 NaCl, 4.7 KCl, 1.2 $MgSO_4$, 1.2 KH_2PO_4, 1.2 $CaCl_2$, 10 glucose, 25 $NaHCO_3$, pH 7.4) or low Na^+ Krebs buffer with equimolar NMDG-Cl substituted for NaCl for 24 h. The *bar graph* represents the percentage of number of cells in each cell cycle phase for different experimental conditions. Data are representative of six independent experiments. *B,* expression of $p21^{Cip1}$ ($n \geq 5$) and $p27^{kip1}$ ($n \geq 4$) was determined in wild type D54MG cells incubated in either control Krebs buffer or low Na^+ Krebs buffer for 24 h after 48 h of serum starvation. Actin was used as a loading control. Each *bar* represents normalized densitometry compared with untransfected D54MG-WT cells. *IB*, immunoblot.

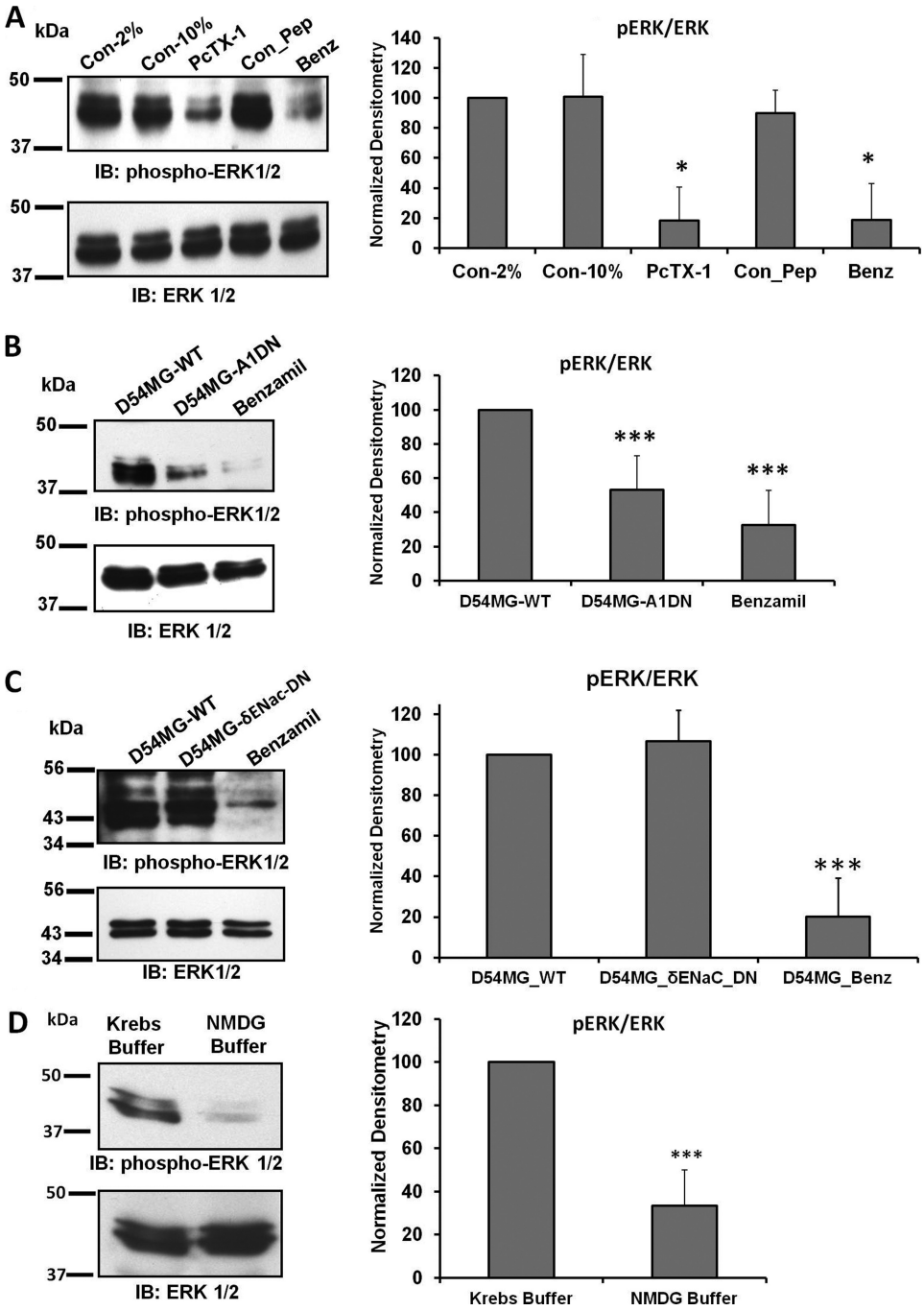

FIGURE 7. **Inhibition of ERK1/2 phosphorylation.** *A,* immunoblot (*IB*) analysis of lysates from D54-MG cells treated with PcTX-1, control peptide (*Con_Pep*), or benzamil (*Benz*) for 24 h. The blots were probed for phospho-ERK1/2 and then stripped and reprobed for total ERK1/2, $n \geq 3$. *Con*, control. *B,* immunoblot analysis of lysates from D54MG-WT, D54MG-A1DN cells, and D54MG-WT + benzamil, $n \geq 6$. *C,* knockdown of δENaC did not affect the phosphorylation of ERK1/2 compared with wild type D54MG cells, $n \geq 4$. In each case, the *bar graph* illustrates the normalized density compared with untreated cells exposed to 2% FBS. *D,* low [Na^+] also down-regulated phosphorylation of ERK1/2 in D54-MG glioma cells following 24 h of incubation. Each *bar* represents the normalized density compared with cells normal Kreb's buffer ($n \geq 4$).

the exception of the changes in p21, which were either not affected or slightly decreased by the blockers. It is possible that p21 is not an essential regulator of the cell cycle in U87 cells, as other studies have shown that p21 is much slower to respond to a variety of experimental maneuvers in this cell type as compared with other glioma cells (supplemental Figs. S3 and S4) (24–27). Real time PCR analysis demonstrated that in all cases the increases in $p21^{Cip1}$ expression were due to an increase in mRNA; in contrast, message levels of $p27^{Kip1}$ were not affected by any experimental maneuver (supplemental Fig. S5).

DISCUSSION

Grade IV gliomas are highly invasive tumors, distinguished by their ability to migrate through the brain parenchyma to establish secondary foci distant from the primary tumor. Multiple laboratories have reported that ion transport plays a critical role in both migration and proliferation of glioma cells, and

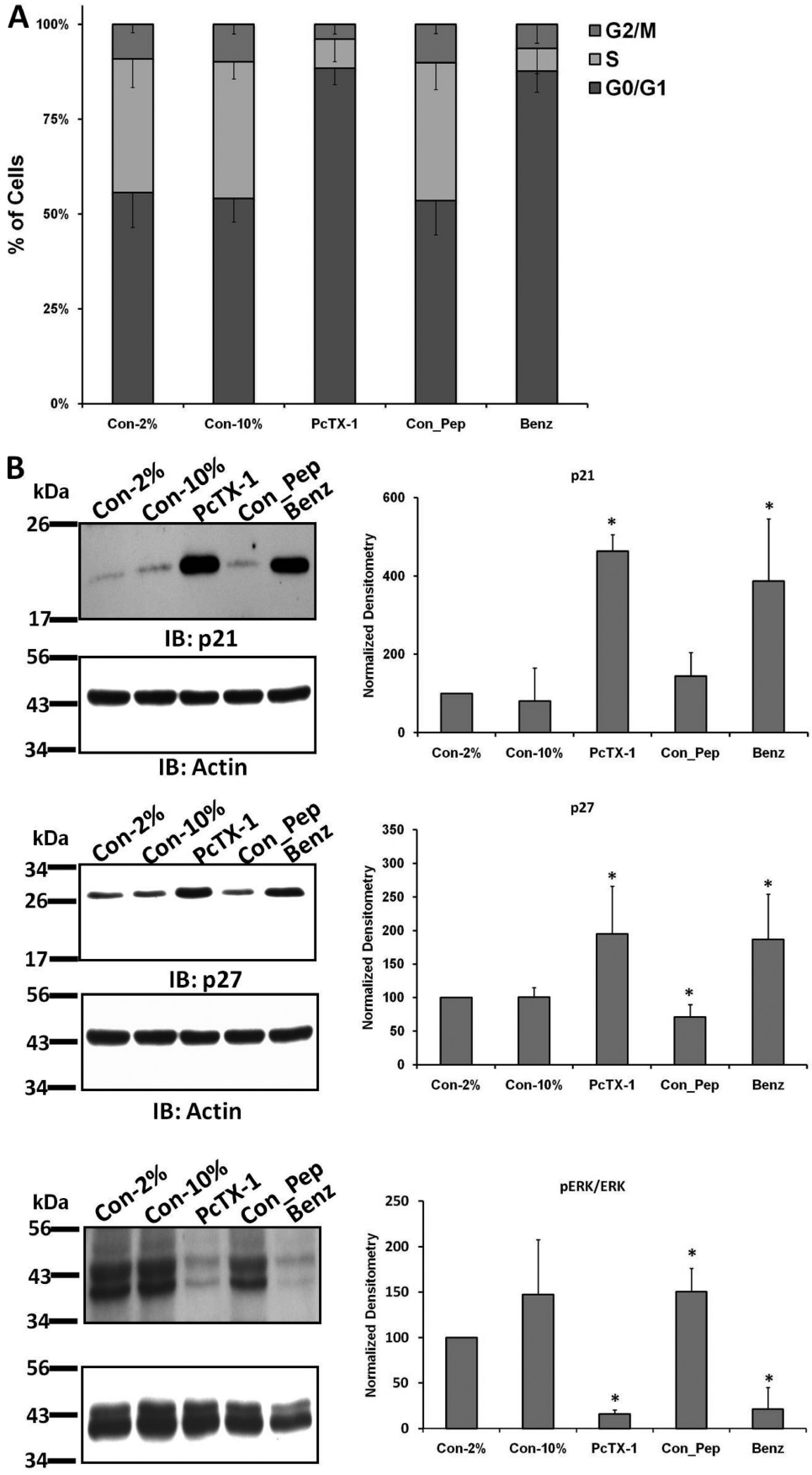
A
100%
75%
50%
25%
0%
% of Cells
G2/M
S
G0/G1
Con-2%
Con-10%
PcTX-1
Con_Pep
Benz
B
kDa
Con-2%
Con-10%
PcTX-1
Con_Pep
Benz
26
17
IB: p21
56
43
34
IB: Actin
p21
Normalized Densitometry
600
400
200
0
Con-2%
Con-10%
PcTX-1
Con_Pep
Benz
34
26
17
IB: p27
56
43
34
IB: Actin
p27
Normalized Densitometry
350
300
250
200
150
100
50
0
56
43
34
pERK/ERK
Normalized Densitometry
250
200
150
100
50
0

potassium, chloride, calcium, and voltage-gated sodium channels have all been implicated (1, 28, 29). Earlier studies proposed that Na^+ influx was itself a mitogenic signal, initiating cell cycle progression in neuroblastoma-glioma hybrid cells, as inhibitors of sodium transport reduced the DNA synthesis required for cell proliferation (30, 31). Furthermore, the sodium gradient established by the Na^+/K^+-ATPase is importantly used to drive uptake of metabolic substrates such as glucose and amino acids, as well as to remove harmful metabolites such as H^+ via turnover of the Na^+/H^+ exchanger (NHE). Cells can also control their internal volume by regulating transport of Na^+, K^+, and Cl^- across the plasma membrane, swelling or shrinking as required. Although much less sensitive to amiloride than the prototypical renal sodium channel $\alpha\beta\gamma$ENaC ($K_i^{amil} < 0.1$ μM (32)), the glioma cation channel that we have identified is critically involved in migration and proliferation (13–16). This channel is inhibited by amiloride and its analogs and is blocked by PcTX-1, to which it is exquisitely sensitive (K_i^{amil} 10–100 μM; $K_i^{PcTX\text{-}1} K_i \sim 40$ pM (17)). This peptide exhibits high specificity for ASIC1, with no effect on ASIC2, heteromers of ASIC subunits, or $\alpha\beta\gamma$ENaC (18). However, PcTX-1 prevented a regulatory volume increase in glioma cells following a hyperosmotic challenge (19). It has previously been suggested that in addition ENaC plays an important role in wound healing (33, 34) and proliferation (35). Both ASIC and ENaC channels contribute to migration of vascular smooth muscle cells (36, 37), although in neither case are the underlying mechanisms well understood.

In this study, we have begun to dissect out these mechanisms by examining the effect of current inhibition on cell cycle intermediates and the MAPK pathway. The cell cycle is a tightly regulated process that is involved in growth, division, and differentiation. It is regulated by both cyclin-dependent kinases and inhibitor proteins, including $p21^{Cip1}$ and $p27^{Kip1}$ (38, 39). We found that expression of these CKI proteins was up-regulated when the glioma current was inhibited under all conditions tested. This was specific to the glioma conductance, as knocking down δENaC had no effect on CKI expression. Expression of $p21^{Cip1}$ and $p27^{Kip1}$ is primarily regulated by transcriptional and post-translational mechanisms, respectively (40), and this was confirmed by our real time PCR results, which showed an increased level of mRNA for $p21^{Cip1}$ but not $p27^{Kip1}$ in every condition where we found up-regulation of protein expression (supplemental Fig. 5). It should be noted that consistent with expression of a nonselective cation channel, we found that the outward K^+ currents were also blocked by PcTX-1 as well as by benzamil, suggesting that K^+ efflux from cells was also inhibited (17). Similar accumulation of these two CKI proteins was found in oligodendrocyte precursors under conditions of K^+ channel block, and it was suggested that the underlying mechanism involved a change in membrane potential (41). However, we observed little change in reversal potential in the presence of benzamil or PcTX-1 in our studies (Fig. 2), suggesting that membrane potential is unlikely to be a key trigger. Expression of $p21^{Cip1}$ was associated with increased mRNA, consistent with the expression of wild type p53 in D54-MG cells (42, 43). The dissociation between $p27^{Kip1}$ accumulation and mRNA may reflect rapid turnover of message, increased translation, or increased protein stability (44).

Our finding that ASIC-1-mediated glioma cell cycle arrest was associated with increased expression of CKIs prompted us to examine the involvement of the MAPK pathway by evaluating the phosphorylation status of ERK1/2. Activation of ERK1/2 is classically downstream of the EGFR, which is overexpressed in most GBM tumors (45), and ERK1/2 phosphorylation is a key signaling event controlling migration and proliferation of multiple cancer cells, including gliomas (10, 23, 46). However, activation of ERK1/2 in the absence of EGFR amplification has been reported, suggesting that nonclassical pathways are also involved in the regulation of this important transcriptional regulator (45). Down-regulation of ERK1/2 is intimately associated with cell cycle inhibition and accumulation of $p27^{Kip1}$ (47, 48) and $p21^{Cip1}$ (49). ERK is also a potent regulator of glioma cell migration; inhibition of Rho-associated kinase reduced phosphorylation of ERK1/2 and decreased cell migration (50). Several transporter proteins are also targets of ERK1/2 phosphorylation. ERK phosphorylates β- and γENaC, increasing retrieval of $\alpha\beta\gamma$ENaC from the membrane (12, 51) and thus decreasing current. However, we have now demonstrated the reciprocal relationship in the glioma cell, as down-regulating the Na^+ current inhibited phosphorylation of ERK1/2. ERK activation also stimulates turnover of the NHE, which is widely implicated in tumor growth and proliferation (52). This exchanger normally operates to maintain pH_i homeostasis, although in gliomas this protein is up-regulated, and the pH_i is quite alkaline (53). The NHE is effectively inhibited by 100 μM amiloride, and although we used 100 μM benzamil, a less potent amiloride analog as a positive control (54), it is likely that the effects of benzamil are attributable to inhibition of both the glioma cation conductance and NHE. However, inhibition of NHE does not account for the effects of ASIC1 knockdown on CKI accumulation and ERK phosphorylation, suggesting a less prominent role for NHE in this system.

In summary, we have shown that blocking of plasma membrane cation channel complex inhibits migration and proliferation of glioma cells. At the least, this most likely involves inhibition of ERK1/2 phosphorylation and subsequent accumulation of the CKI proteins $p21^{Cip1}$ and $p27^{Kip1}$. How changes in channel activity are transduced to the MAPK pathway remains to be determined.

Acknowledgments—We thank Melissa McCarthy for excellent cell culture assistance and Drs. Yancey Gillespie, Edlira Clark, Niren Kapoor, and Yawar Qadri for helpful discussions.

FIGURE 8. **Inhibition of glioma conductance caused cell cycle arrest and decreased phosphorylation of ERK1/2 in primary GBM cells.** *A, stacked bar graph* represents the percentage of primary GBM cells in each cell cycle phase under different experimental conditions, $n \geq 6$. *B,* expression of $p21^{Cip1}$ and $p27^{Kip1}$ and level of phospho-ERK1/2 in primary GBM cells treated with 100 nM PcTX-1, control peptide (*Con_Pep*), or 100 μM benzamil (*Benz*) for 24 h. *Con*, control. Each *bar* represents the normalized densitometry compared with control in 2% FBS, $n \geq 5$ for each. *IB*, immunoblot.

REFERENCES

1. Kunzelmann, K. (2005) Ion channels and cancer. *J. Membr. Biol.* **205,** 159–173
2. Roderick, H. L., and Cook, S. J. (2008) Ca^{2+} signaling checkpoints in cancer. Remodeling Ca^{2+} for cancer cell proliferation and survival. *Nat. Rev. Cancer* **8,** 361–375
3. Soroceanu, L., Manning, T. J., Jr., and Sontheimer, H. (1999) Modulation of glioma cell migration and invasion using Cl(−) and K(+) ion channel blockers. *J. Neurosci.* **19,** 5942–5954
4. Prevarskaya, N., Zhang, L., and Barritt, G. (2007) TRP channels in cancer. *Biochim. Biophys. Acta* **1772,** 937–946
5. Ullrich, N., Gillespie, G. Y., and Sontheimer, H. (1996) Human astrocytoma cells express a unique chloride current. *Neuroreport* **7,** 1020–1024
6. Wang, Z. (2004) Roles of K^+ channels in regulating tumor cell proliferation and apoptosis. *Pflugers Arch.* **448,** 274–286
7. Chioni, A. M., Brackenbury, W. J., Calhoun, J. D., Isom, L. L., and Djamgoz, M. B. (2009) A novel adhesion molecule in human breast cancer cells. Voltage-gated Na^+ channel β1 subunit. *Int. J. Biochem. Cell Biol.* **41,** 1216–1227
8. Ransom, C. B., O'Neal, J. T., and Sontheimer, H. (2001) Volume-activated chloride currents contribute to the resting conductance and invasive migration of human glioma cells. *J. Neurosci.* **21,** 7674–7683
9. Fanton, C. P., McMahon, M., and Pieper, R. O. (2001) Dual growth arrest pathways in astrocytes and astrocytic tumors in response to Raf-1 activation. *J. Biol. Chem.* **276,** 18871–18877
10. McLendon, R. E., Turner, K., Perkinson, K., and Rich, J. (2007) Second messenger systems in human gliomas. *Arch. Pathol. Lab. Med.* **131,** 1585–1590
11. Falin, R. A., and Cotton, C. U. (2007) Acute down-regulation of ENaC by EGF involves the PY motif and putative ERK phosphorylation site. *J. Gen. Physiol.* **130,** 313–328
12. Soundararajan, R., Melters, D., Shih, I. C., Wang, J., and Pearce, D. (2009) Epithelial sodium channel regulated by differential composition of a signaling complex. *Proc. Natl. Acad. Sci. U.S.A.* **106,** 7804–7809
13. Berdiev, B. K., Xia, J., McLean, L. A., Markert, J. M., Gillespie, G. Y., Mapstone, T. B., Naren, A. P., Jovov, B., Bubien, J. K., Ji, H. L., Fuller, C. M., Kirk, K. L., and Benos, D. J. (2003) Acid-sensing ion channels in malignant gliomas. *J. Biol. Chem.* **278,** 15023–15034
14. Bubien, J. K., Keeton, D. A., Fuller, C. M., Gillespie, G. Y., Reddy, A. T., Mapstone, T. B., and Benos, D. J. (1999) Malignant human gliomas express an amiloride-sensitive Na^+ conductance. *Am. J. Physiol.* **276,** C1405–C1410
15. Kapoor, N., Bartoszewski, R., Qadri, Y. J., Bebok, Z., Bubien, J. K., Fuller, C. M., and Benos, D. J. (2009) Knockdown of ASIC1 and epithelial sodium channel subunits inhibits glioblastoma whole cell current and cell migration. *J. Biol. Chem.* **284,** 24526–24541
16. Vila-Carriles, W. H., Kovacs, G. G., Jovov, B., Zhou, Z. H., Pahwa, A. K., Colby, G., Esimai, O., Gillespie, G. Y., Mapstone, T. B., Markert, J. M., Fuller, C. M., Bubien, J. K., and Benos, D. J. (2006) Surface expression of ASIC2 inhibits the amiloride-sensitive current and migration of glioma cells. *J. Biol. Chem.* **281,** 19220–19232
17. Bubien, J. K., Ji, H. L., Gillespie, G. Y., Fuller, C. M., Markert, J. M., Mapstone, T. B., and Benos, D. J. (2004) Cation selectivity and inhibition of malignant glioma Na^+ channels by Psalmotoxin 1. *Am. J. Physiol. Cell Physiol.* **287,** C1282–C1291
18. Escoubas, P., De Weille, J. R., Lecoq, A., Diochot, S., Waldmann, R., Champigny, G., Moinier, D., Ménez, A., and Lazdunski, M. (2000) Isolation of a tarantula toxin specific for a class of proton-gated Na^+ channels. *J. Biol. Chem.* **275,** 25116–25121
19. Ross, S. B., Fuller, C. M., Bubien, J. K., and Benos, D. J. (2007) Amiloride-sensitive Na^+ channels contribute to regulatory volume increases in human glioma cells. *Am. J. Physiol. Cell Physiol.* **293,** C1181–C1185
20. Akaike, N., and Harata, N. (1994) Nystatin perforated patch recording and its applications to analyses of intracellular mechanisms. *Jpn. J. Physiol.* **44,** 433–473
21. Sherr, C. J., and Roberts, J. M. (1999) CDK inhibitors. Positive and negative regulators of G_1-phase progression. *Genes Dev.* **13,** 1501–1512
22. Haerteis, S., Krueger, B., Korbmacher, C., and Rauh, R. (2009) The δ-subunit of the epithelial sodium channel (ENaC) enhances channel activity and alters proteolytic ENaC activation. *J. Biol. Chem.* **284,** 29024–29040
23. Nakabayashi, H., and Shimizu, K. (2011) HA1077, a Rho kinase inhibitor, suppresses glioma-induced angiogenesis by targeting the Rho-ROCK and the mitogen-activated protein kinase kinase/extracellular signal-regulated kinase (MEK/ERK) signal pathways. *Cancer Sci.* **102,** 393–399
24. Jia, L., Soengas, M. S., and Sun, Y. (2009) ROC1/RBX1 E3 ubiquitin ligase silencing suppresses tumor cell growth via sequential induction of G_2-M arrest, apoptosis, and senescence. *Cancer Res.* **69,** 4974–4982
25. Komata, T., Kanzawa, T., Takeuchi, H., Germano, I. M., Schreiber, M., Kondo, Y., and Kondo, S. (2003) Antitumour effect of cyclin-dependent kinase inhibitors (p16(INK4A), p18(INK4C), p19(INK4D), p21(WAF1/CIP1), and p27(KIP1)) on malignant glioma cells. *Br. J. Cancer* **88,** 1277–1280
26. Wang, K., Pan, L., Che, X., Cui, D., and Li, C. (2010) Gli1 inhibition induces cell cycle arrest and enhanced apoptosis in brain glioma cell lines. *J. Neurooncol.* **98,** 319–327
27. Xu, J., Sampath, D., Lang, F. F., Prabhu, S., Rao, G., Fuller, G. N., Liu, Y., and Puduvalli, V. K. (2011) Vorinostat modulates cell cycle regulatory proteins in glioma cells and human glioma slice cultures. *J. Neurooncol.* **105,** 241–251
28. Cuddapah, V. A., and Sontheimer, H. (2011) Ion channels and transporters in cancer. 2. Ion channels and the control of cancer cell migration. *Am. J. Physiol. Cell Physiol.* **301,** C541–549
29. Joshi, A. D., Parsons, D. W., Velculescu, V. E., and Riggins, G. J. (2011) Sodium ion channel mutations in glioblastoma patients correlate with shorter survival. *Mol. Cancer* **10,** 17
30. O'Donnell, M. E., Cragoe, E., Jr., and Villereal, M. L. (1983) Inhibition of Na^+ influx and DNA synthesis in human fibroblasts and neuroblastoma-glioma hybrid cells by amiloride analogs. *J. Pharmacol. Exp. Ther.* **226,** 368–372
31. O'Donnell, M. E., and Villereal, M. L. (1982) Membrane potential and sodium flux in neuroblastoma X glioma hybrid cells. Effects of amiloride and serum. *J. Cell. Physiol.* **113,** 405–412
32. Kellenberger, S., and Schild, L. (2002) Epithelial sodium channel/degenerin family of ion channels. A variety of functions for a shared structure. *Physiol. Rev.* **82,** 735–767
33. Chifflet, S., Hernández, J. A., and Grasso, S. (2005) A possible role for membrane depolarization in epithelial wound healing. *Am. J. Physiol. Cell Physiol.* **288,** C1420–C1430
34. Del Mónaco, S. M., Marino, G. I., Assef, Y. A., Damiano, A. E., and Kotsias, B. A. (2009) Cell migration in BeWo cells and the role of epithelial sodium channels. *J. Membr. Biol.* **232,** 1–13
35. Bondarava, M., Li, T., Endl, E., and Wehner, F. (2009) α-ENaC is a functional element of the hypertonicity-induced cation channel in HepG2 cells, and it mediates proliferation. *Pflugers Arch.* **458,** 675–687
36. Grifoni, S. C., Gannon, K. P., Stec, D. E., and Drummond, H. A. (2006) ENaC proteins contribute to VSMC migration. *Am. J. Physiol. Heart Circ. Physiol.* **291,** H3076–H3086
37. Grifoni, S. C., Jernigan, N. L., Hamilton, G., and Drummond, H. A. (2008) ASIC proteins regulate smooth muscle cell migration. *Microvasc. Res.* **75,** 202–210
38. George, J., Banik, N. L., and Ray, S. K. (2010) Knockdown of hTERT and concurrent treatment with interferon-γ inhibited proliferation and invasion of human glioblastoma cell lines. *Int. J. Biochem. Cell Biol.* **42,** 1164–1173
39. Herrero-González, S., Gangoso, E., Giaume, C., Naus, C. C., Medina, J. M., and Tabernero, A. (2010) Connexin43 inhibits the oncogenic activity of c-Src in C6 glioma cells. *Oncogene* **29,** 5712–5723
40. Slingerland, J., and Pagano, M. (2000) Regulation of the cdk inhibitor p27 and its deregulation in cancer. *J. Cell. Physiol.* **183,** 10–17
41. Ghiani, C. A., Yuan, X., Eisen, A. M., Knutson, P. L., DePinho, R. A., McBain, C. J., and Gallo, V. (1999) Voltage-activated K^+ channels and membrane depolarization regulate accumulation of the cyclin-dependent kinase inhibitors p27(Kip1) and p21(CIP1) in glial progenitor cells. *J. Neurosci.* **19,** 5380–5392
42. Gomez-Manzano, C., Fueyo, J., Kyritsis, A. P., Steck, P. A., Roth, J. A.,

McDonnell, T. J., Steck, K. D., Levin, V. A., and Yung, W. K. (1996) Adenovirus-mediated transfer of the p53 gene produces rapid and generalized death of human glioma cells via apoptosis. *Cancer Res.* **56,** 694–699
43. Jung, Y. S., Qian, Y., and Chen, X. (2010) Examination of the expanding pathways for the regulation of p21 expression and activity. *Cell. Signal.* **22,** 1003–1012
44. Vervoorts, J., and Lüscher, B. (2008) Post-translational regulation of the tumor suppressor p27(KIP1). *Cell. Mol. Life Sci.* **65,** 3255–3264
45. Lopez-Gines, C., Gil-Benso, R., Benito, R., Mata, M., Pereda, J., Sastre, J., Roldan, P., Gonzalez-Darder, J., and Cerdá-Nicolás, M. (2008) The activation of ERK1/2 MAP kinases in glioblastoma pathobiology and its relationship with EGFR amplification. *Neuropathology* **28,** 507–515
46. Glassmann, A., Reichmann, K., Scheffler, B., Glas, M., Veit, N., and Probstmeier, R. (2011) Pharmacological targeting of the constitutively activated MEK/MAPK-dependent signaling pathway in glioma cells inhibits cell proliferation and migration. *Int. J. Oncol.* **39,** 1567–1575
47. Gysin, S., Lee, S. H., Dean, N. M., and McMahon, M. (2005) Pharmacologic inhibition of RAF→MEK→ERK signaling elicits pancreatic cancer cell cycle arrest through induced expression of p27Kip1. *Cancer Res.* **65,** 4870–4880
48. Kortylewski, M., Heinrich, P. C., Kauffmann, M. E., Böhm, M., MacKiewicz, A., and Behrmann, I. (2001) Mitogen-activated protein kinases control p27/Kip1 expression and growth of human melanoma cells. *Biochem. J.* **357,** 297–303
49. Hwang, C. Y., Lee, C., and Kwon, K. S. (2009) Extracellular signal-regulated kinase 2-dependent phosphorylation induces cytoplasmic localization and degradation of p21Cip1. *Mol. Cell. Biol.* **29,** 3379–3389
50. Zohrabian, V. M., Forzani, B., Chau, Z., Murali, R., and Jhanwar-Uniyal, M. (2009) Rho/ROCK and MAPK signaling pathways are involved in glioblastoma cell migration and proliferation. *Anticancer Res.* **29,** 119–123
51. Yang, L. M., Rinke, R., and Korbmacher, C. (2006) Stimulation of the epithelial sodium channel (ENaC) by cAMP involves putative ERK phosphorylation sites in the C termini of the channel's β- and γ-subunit. *J. Biol. Chem.* **281,** 9859–9868
52. Slepkov, E. R., Rainey, J. K., Sykes, B. D., and Fliegel, L. (2007) Structural and functional analysis of the Na^+/H^+ exchanger. *Biochem. J.* **401,** 623–633
53. McLean, L. A., Roscoe, J., Jorgensen, N. K., Gorin, F. A., and Cala, P. M. (2000) Malignant gliomas display altered pH regulation by NHE1 compared with nontransformed astrocytes. *Am. J. Physiol. Cell Physiol.* **278,** C676–C688
54. Nakamura, K., Kamouchi, M., Kitazono, T., Kuroda, J., Matsuo, R., Hagiwara, N., Ishikawa, E., Ooboshi, H., Ibayashi, S., and Iida, M. (2008) Role of NHE1 in calcium signaling and cell proliferation in human CNS pericytes. *Am. J. Physiol. Heart Circ. Physiol.* **294,** H1700–H1707